

Development of Quadruped Achieving High Terrain Adaptability (DOF Configuration Consideration for Redundant Leg Structures)

Takuya KITAMURA*¹ and Yusuke OTA*¹

*¹ Department of Advanced Robotics, Chiba Institute of Technology
2-17-1 Tsudanuma, Narasino-shi, Chiba 275-0016, JAPAN
s0926047@gmail.co.jp, yusuke.ohata@it-chiba.ac.jp

Abstract

Legged locomotion is suitable to move on uneven terrain. However, advantages of legged robots have not been achieved yet. In this study, a relationship between combinations of the joints and generated force or torque will be discussed. Legs with four joints were considered. These legs have a possibility to adapt a rough terrain because of their redundancy. Redundant joint can change the direction of maximum output force without changing output force distribution. After several considerations, three legs out of 81 combinations are examined to simulate. Output force distributions during walking on flat ground and slope are reported.

Keywords: quadruped robot, DOF configuration

1 Introduction

Walking robots have the notable advantage of selecting their footing points. As compared with other moving robot, such as wheeled robots [1] or snake-style robots [2], this advantage allows the superiority of traversing rough-terrain fields including steps, ditches and obstacles. Walking robots with multiple legs can maintain their static balance while moving. In quadruped robots, for example three legs have been used to keep their body posture while one leg has been swung forward for movements. Many quadrupeds have legs with three degrees of freedom (DOF) in order to locate their foot arbitrarily three-dimensional environments. To overcome large steps, however, beside the selection of foot landing points, generation and control of foot forces applied on the ground should be considered for effective weight shifting of movements. Leg joints should be suitably configured for step climbing, so that quadruped robots can walk without losing their balance. The mobility of walking robots on rough terrain has deep dependency on the DOF configuration of their legs.

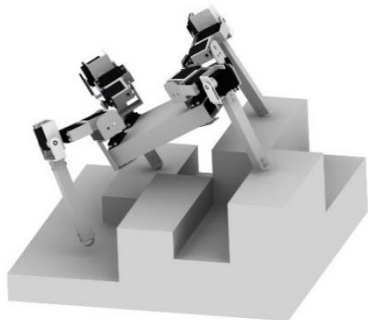


Fig. 1 The quadruped climbing on high step terrain

In the literature, a number of approaches for large-step climbing can be found, mostly featured by

- 1) Extendable legs. An extend leg mechanism makes static stability to increase on slope or uneven terrain [3].
- 2) Active ankle joints. Many walking robots are designed without ankle joints or with passive ankle joints under the pre-assumption that foot of quadruped robots contacts on the ground at a point. If ankle joints are made active, these joints can generate torques for movements [4].
- 3) Intermittent crawl gait. The intermittent crawl gait can increase the static stability during the moving slopes. That is the gait to swing the center of gravity (CG) of the robot sideways when all four legs are grounded [5].
- 4) Inverse trapezoid posture. When quadruped robots move on steps, the trajectories of their CGs have discontinuous velocities. Using inverse trapezoid posture, the footprint width of forward legs makes wider and that of hind legs makes narrower, improves continuity of moving velocity [6].

The relation between the moving performance of walking robots and the DOF configuration of legs has been investigated vigorously. Roennau et al. realized uneven-terrain walking by their hexapod “LAURON V” [7]. LAURON V, imitating a stick insect, has six legs composed by four joint. Hodoshima et al. developed “ASURA I” [8], imitating a harvestman, and it has six legs of four joint. Fujie et al. proposed a walking procedure to minimize the necessary joint torque and energy consumption for a 4-DOF-leg quadruped robot [9]. Maufroy et al. designed a mammal-style quadruped robot “KOTETSU” [10]. This robot has 4-DOF legs and achieved superior force generating characteristics. Hirose and Tsukagoshi researched the quadruped “TITAN-VII” [3], where its extendable leg mechanism can be maintain the CG in stable position during steep slope locomotion.

The primary difficulty in moving on large steps is at appropriate generation and control of moving forces applied by feet on the ground. Although 3-DOF legs can generate ground-kicking forces in any directions, the direction of its maximum force cannot be flexibly controlled. The changed of the body posture involved to be adequately controlled. In the designing process of quadruped robots, their legs are usually designed to walk on the flat ground with the forces on the reachable range of foot motions. Even in that case, available foot forces can be enough for small steps. However, for much higher

steps, more careful considerations of foot forces in terms of both magnitude and direction are inevitably required. With large-torque actuators, large kicking force can be also available for robot movements. Such actuators are heavier normally, and the heavy weight of robots deteriorates the moving performance and the adaptability to irregular fields. It is desired to establish an approach of enhancing the walking the walking performance without enlarging the robot weight.

From the discussions above, we have proposed a methodology to develop quadruped robots, which have four-joint legs unlike usual three joints. The redundancy in leg joints is effectively used to generate the ground-kicking force in terms of magnitude and direction. The adaptability of quadruped walking robots on rough terrains will be increased by clarifying the relation between the joint configuration, the feasible range of foot motions, and the available force generated by legs. In this paper, a quadruped walking robot that can walk on high steps and large-scaled uneven terrains is focused, and the effective use of the redundancy in the leg joint configuration is discussed.

2 DOF configuration

Quadruped robot has usually three-DOF per leg, 12 DOF in total. Each leg can select an arbitrary position of foot placement inside its workspace. In case one DOF is added to the 3-DOF leg, that leg can control its 3-DOF as positions and one-DOF as a posture. In this chapter, the DOF configuration of 4-DOF leg is considered. It is assumed that all the joints consist of one-DOF structure, which can rotate around the roll axis (x -axis), the pitch axis (y -axis) and the yaw axis (z -axis), as shown in Fig. 2. Any leg which several-DOF joints can be simulated by combination of these three joints. Legs which can generate 4-DOF motion should be combined the three joints. Then all the DOF combinations possibilities for the legs becomes $3^4 = 81$ combinations. From the 81 combinations of the leg, appropriate DOF configurations of the leg should be selected as for a large scale uneven terrain walking quadruped design. Next, the legs generate the same DOF configurations, as shown in Fig. 3, are removed. Three configuration legs derived from the simulations are shown in Fig. 3, however, all the legs generate the same motion. That is because the roll joint attached after the yaw axis makes as the same motion as the pitch joint after the yaw axis generates, which is the same DOF configuration after 90-degree rotation of the yaw axis from the original configurations. In this study, the leg must ground at a point. Then, the combinations that the fourth joint is consisted of the joint with the yaw axis rotation are removed from the consideration because that rotational joint makes local motion, not to generate any motion toward the global coordinates but to rotate only shank linkage itself. That is also the same situation when two yaw axis rotational joints are connected in series. These cases are removed from above simulation. Then 81 combinations of leg DOF configurations can be reduced to 16. Finally, necessary conditions as the legs of walking robot is considered, as follows;

- Possibility of taking a leg trajectory for walking
- Ability of changing a leg posture as much as possible

All the 16 quadrupeds with each simulated legs are considered. Here, four legs of the quadruped robot are constructed by the same DOF configuration leg. Then, only five configured legs are remained as use of the leg for quadruped robot, as is shown in Fig. 4.

Several quadrupeds, which imitate insects and have insect-style DOF configuration, have been researched until now so as to acquire a higher terrain adaptability rather than mammal-style configuration. Our quadruped will be also developed based on the insect-style joint configuration in order to achieve high terrain adaptability. Then, the simulation strategy is considered that one joint is added to the leg with insect-style joint configuration. These legs consist of three rotational joints, that is the yaw-roll-roll joints are serially connected from its body, and four links connected each joint and body. Therefore one additional joint in our simulation is positioned one link out of its four links. The number of combinations reaches 12 ($=3 \times 4$ combinations). As applying the same manner, the considered legs with the same joint configuration after 90-degree rotation of yaw joint are reduced to six. As a result to compare the remained both considerations, three legs are founded to have the same joint configurations of the leg, that is shown in Fig. 5. From here, each model is named as Model 1 in Fig. 5 (a), Model 2 in Fig. 5 (b) and Model 3 in Fig. 5 (c).

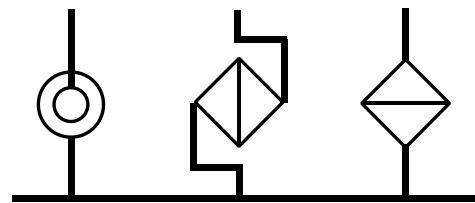


Fig. 2 Roll, pith and yaw joints

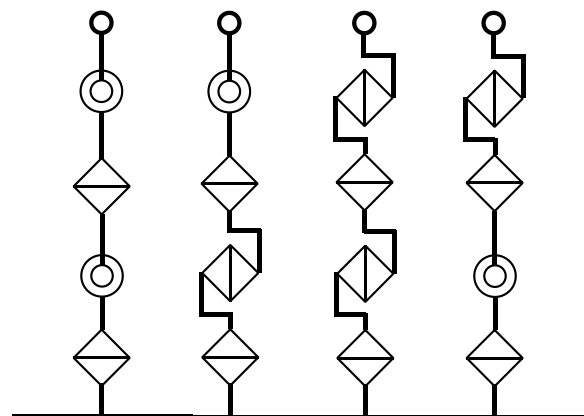


Fig. 3 Same models of the DOF configuration

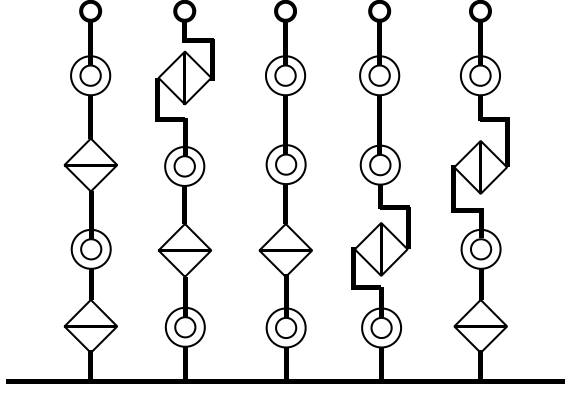


Fig. 4 Selected leg models

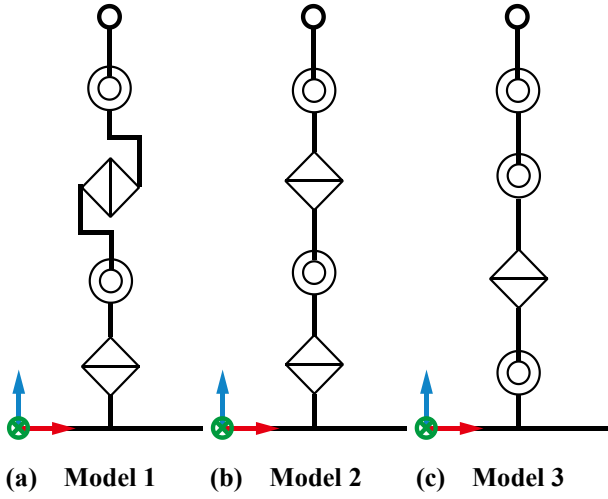


Fig. 5 Joints alignments for simulation

3 Kinematics

3.1 Forward kinematics

The relation between the joint angles and the foot position is first derived by forward kinematics. For three models above, coordinate systems are set as shown in Figs. 6(a), 6(b) and 6(c), where joints in each leg are numbered from the base (body), and joint angles and link lengths are labeled as θ_1 to θ_4 and as L_1 to L_5 , respectively. The n -th link connects the $(n-1)$ -th joint to the n -th joint, and the global coordinate system for each leg is attached at the 0-th joint on the body. The foot position and the leg posture can be calculated by the well-known DH method with these setting through homogeneous transformations.

3.2 Inverse kinematics

For each leg model consisting of 4-DOFs, the Jacobian matrix can be derived by partially differentiating the foot position with respect to the joint angles. The inverse of the resulting 3-by-4 Jacobian matrix cannot be computed directly. Therefore, a pseudo-inverse matrix, where the square sum of all the joint angular velocities is minimized, is adopted for the subsequent evaluation. The pseudo-inverse matrix is defined as below.

$$J = \begin{bmatrix} \frac{\partial x}{\partial \theta_1} & \frac{\partial x}{\partial \theta_2} & \frac{\partial x}{\partial \theta_3} & \frac{\partial x}{\partial \theta_4} \\ \frac{\partial y}{\partial \theta_1} & \frac{\partial y}{\partial \theta_2} & \frac{\partial y}{\partial \theta_3} & \frac{\partial y}{\partial \theta_4} \\ \frac{\partial z}{\partial \theta_1} & \frac{\partial z}{\partial \theta_2} & \frac{\partial z}{\partial \theta_3} & \frac{\partial z}{\partial \theta_4} \end{bmatrix} \quad (1)$$

$$J^+ = J^T (JJ^T)^{-1} \quad (2)$$

$$\dot{q} = J^+ \dot{r} + (I - J^+ J) k \quad (3)$$

Here, J^T and J^+ show a transpose and a pseudo-inverse of Jacobian matrix, and I and k are a unit vector a weight vectors, respectively. The four-dimensional joint angle vectors θ can be obtained by numerically integrating the joint angular velocity vector $\dot{\theta}$, with Eq. (3) using MATLAB.

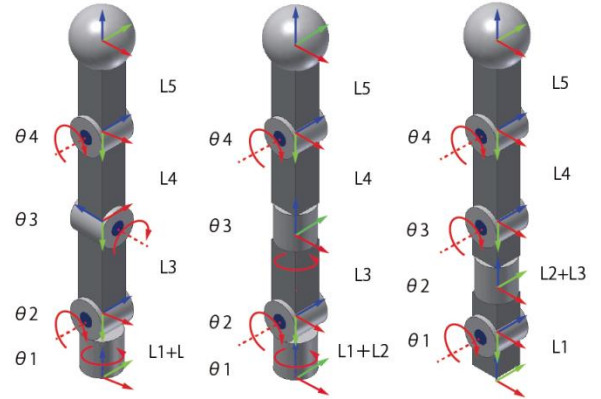


Fig. 6 Parameters and coordinates of each model

4 Force generation analysis

Legs of walking robots should generate enough force both to support self-weight and to move its body forward. The output force is analyzed in case of three models which mentioned above.

4.1 Output force to Z-direction in workspace

Static force that is generated by the robot is analyzed. Relationship between joint torque and output force can be described as follows.

$$\tau = J^T F \quad (4)$$

$$F = (J^T)^{-1} \tau \quad (5)$$

Here, all the links L_1 , L_2 , L_3 , L_4 and L_5 in the model 1, 2 and 3 are set as 10. Then, all the joint torques τ_1, τ_2, τ_3 and τ_4 are also regulated as 1. Simulation results to output force toward Z-direction are shown in Figs. 7, 8 and 9. Result shows that the Model 3 has a wider area to generate a large force toward Z-direction.

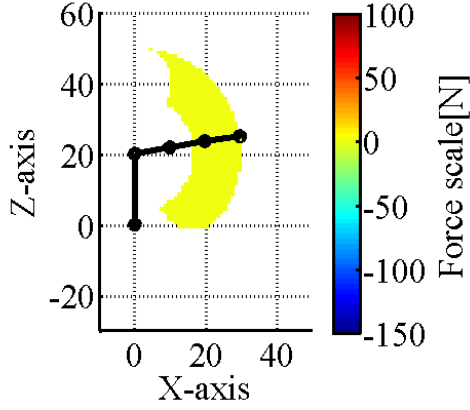


Fig. 7 Output Force to Z-direction of model 1

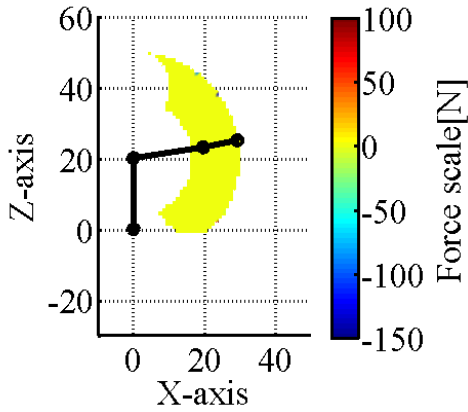


Fig. 8 Output force to Z-direction of model 2

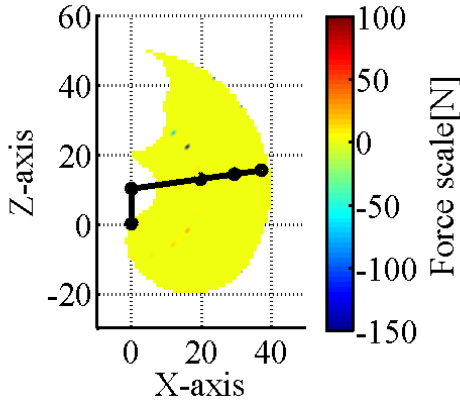


Fig. 9 Output force to Z-direction of model 3

4.2 Force analysis for slope climbing

Necessary force in order to propel the robot body is analyzed. Analyzed legs have redundancy, then not only foot positions, x , y and z , but also leg posture, ψ , can be determined. Therefore output force at some point is changed by leg posture. Maximum output force is analyzed in workspace and the leg posture at the same position should be also analyzed at the same time. The Jacobian matrix of the robot with redundant leg-DOF is modified as below, in case that the joint angle is shown as θ_i (i is the joint number 1~4 shown in Figs. 6 (a), 6(b)

and 6(c.) and leg posture is shown as ψ . The posture angle of the leg ψ is measured from a perpendicular axis of the grounded leg.

$$J = \begin{bmatrix} \frac{\partial x}{\partial \theta_1} & \frac{\partial x}{\partial \theta_2} & \frac{\partial x}{\partial \theta_3} & \frac{\partial x}{\partial \theta_4} \\ \frac{\partial y}{\partial \theta_1} & \frac{\partial y}{\partial \theta_2} & \frac{\partial y}{\partial \theta_3} & \frac{\partial y}{\partial \theta_4} \\ \frac{\partial z}{\partial \theta_1} & \frac{\partial z}{\partial \theta_2} & \frac{\partial z}{\partial \theta_3} & \frac{\partial z}{\partial \theta_4} \\ \frac{\partial \psi}{\partial \theta_1} & \frac{\partial \psi}{\partial \theta_2} & \frac{\partial \psi}{\partial \theta_3} & \frac{\partial \psi}{\partial \theta_4} \end{bmatrix} \quad (6)$$

Using this Jacobian matrix into Eqs. 3 and 4 can calculate the output force of the leg. In this time, the output forces are simulated in case the robot walks on flat ground shown in Fig. 10 and on the slope shown in Figs. 11 and 12. When the robot climbs slopes, it can take two different postures. One is the parallel movement that is the body of the robot take its posture in parallel along the slope, inclined from the flat ground shown in Fig. 11. During climbing slopes, the body posture of the robot horizontally as the same posture angle as that of walking on flat ground, as shown in Fig. 12. In each case shown in Figs. 10, 11 and 12, necessary force conditions to move are expressed as below equations. When the robot walks on flat ground in Fig. 10, the necessary forces F_z and F_y are shown as follows.

$$F_z \geq Mg \quad (7)$$

$$F_y \geq MF_a \quad (8)$$

When the robot walks on the slope as shown in Figs. 11 and 12, necessary forces are shown as follows.

$$F_z \geq Mg + F_a \sin \varphi \quad (9)$$

$$F_y \geq MF_a \cos \varphi \quad (10)$$

Output forces are simulated in order to consider the robot can generate enough force to move in each case. As simulation parameters, the slope angle φ is set as 30° , the robot mass M is 0.05, gravitational acceleration g is 9.806, and necessary acceleration force for propelling the robot F_a is 0.005. Figures 13-20 show the results of numerical simulations. Red line shows the result of Model 1 in Fig. 6 (a), green line; Model 2 in Fig. 6 (b) and blue line; Model 3 in Fig. 6 (c). Black line shows the necessary forces calculated from Eqs. (7) to (10). Results of maximum output forces during leg moves so as to walk on flat ground toward the F_z and F_y is shown in Figs. 13 and 14, respectively. The leg posture change to generate the maximum force to Z-direction at each position is shown in Fig. 15. When the robot climbs the slope with inclined posture as shown in Fig. 11, maximum output forces of F_z and F_y are shown in Figs. 16 and Fig. 17, respectively. Posture changes of the leg which is the same condition as the walking on flat ground is shown in Fig. 15. Figures 13, 14 and 15 show the maximum output force toward Z-direction, Y-direction and posture changes of the leg when leg generates maximum force,

respectively.

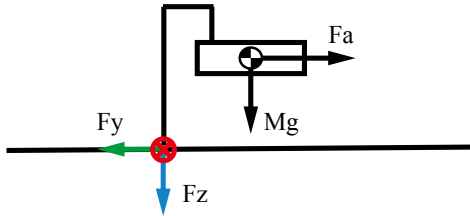


Fig. 10 Necessary force to walk on flat ground

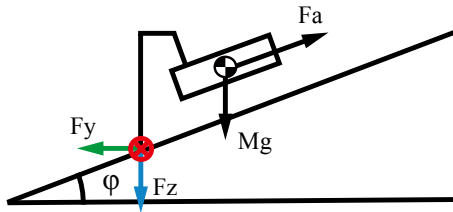


Fig. 11 Necessary force to walk on slope, in robot body inclined along the slope

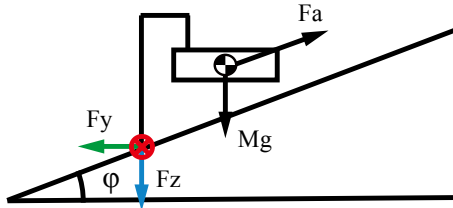


Fig. 12 Necessary force to walk on slope, in robot body keeps horizontal posture

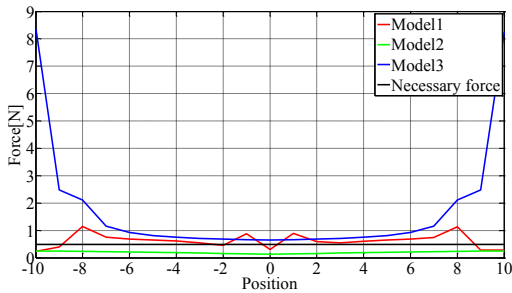


Fig. 13 Maximum F_z distribution moving on flat ground

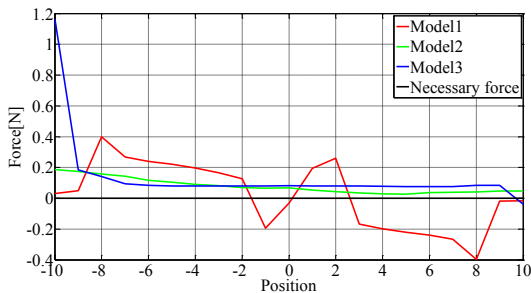


Fig. 14 Maximum F_y distribution moving on flat ground

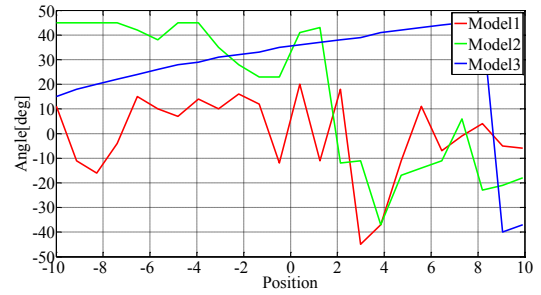


Fig. 15 Leg posture changes at maximum F_z moving on flat ground

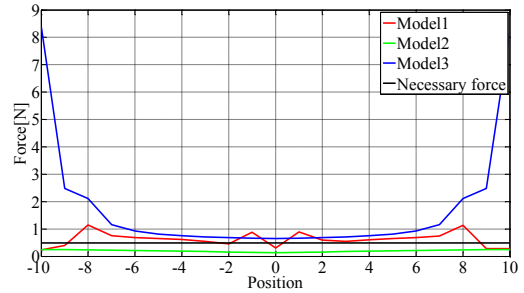


Fig. 16 Maximum F_z distribution moving on a slope taking body posture in Fig. 11

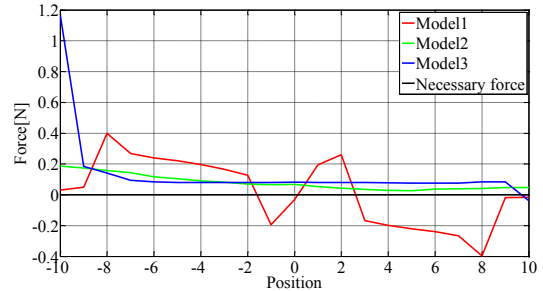


Fig. 17 Maximum F_y distribution moving on slope taking a body posture in Fig. 11

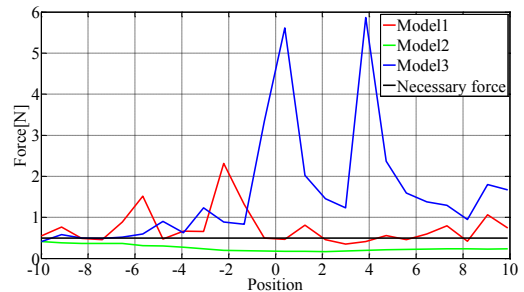


Fig. 18 Maximum F_z distribution moving on slope taking a body posture in Fig. 12

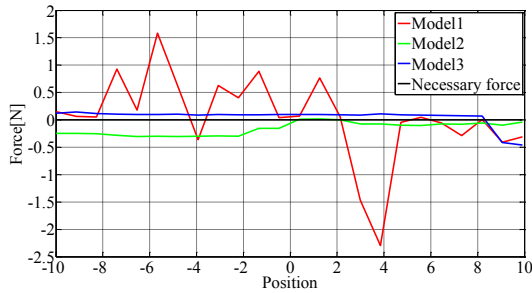


Fig. 19 Maximum F_y distribution moving on slope taking a body posture in Fig. 12

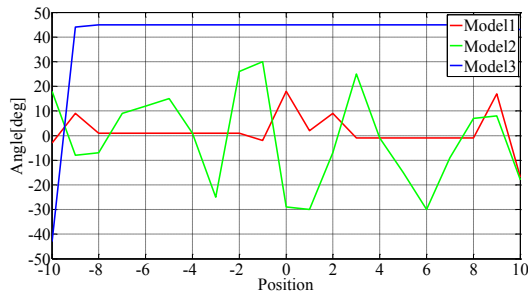


Fig. 20 Leg posture changes at maximum F_z moving on a slope taking body posture in Fig. 12

These results show that the maximum force to support the weight of the robot can be got by Model 1 when the posture of the robot keeps horizontally during walk, and Model 3 can get the maximum force when the posture of the robot inclines till parallel to the slope. These results show that the redundant-DOF can change the directions of the maximum force output. This fact must help the quadruped walking robot walk on uneven terrain efficiently.

5 Conclusions

In this paper, we considered the leg DOF constructions of the quadruped walking robot for large scaled uneven terrain locomotion. Three joint configurations of the leg model with 4-DOF were derived out of 81 combinations, and the generated force characteristics were simulated compared.

We will design a new quadruped with applying this result as a future work.

References

[1] Zhiqing, Li., Shugen, Ma., Bin, Li., Minghui, Wang.,

and Yuechao, Wang., "Parameter Design and Optimization for Mobile Mechanism of a Transformable Wheel-Track Robot", International Conference on Automation and Logistics, (2009), pp.158-163.

- [2] Hirose, S., and Morishima, A., and Tukagosi, S., "Design of Practical Snake Vehicle: Articulated Body Mobile Robot KR-II", International Conference on Advanced Robotics, (1991), pp.833-838.
- [3] Hirose, S., Yoneda, K., and Tsukagoshi, T., "TITAN VII : Quadruped Walking and Manipulating Robot on a Steep Slope", International Conference on Robotics and Automation, (1997), pp.494-500.
- [4] Komatu, H., Ogata, M., Hodoshima, R., Endo, G., Hirose, S., "Development of Quadruped Walking Robot TITAN-XII and Basic Consideration about Mechanics of Large Obstacle Climbing", The 2nd IFToMM ASIAN Conference on Mechanism and Machine Science, (2012), ID112.
- [5] Tsukagoshi, H., Hirose, S., and Yoneda, K., "Maneuvering operations of the quadruped walking robot on the slope", International Conference on Intelligent Robots and System, (1996), pp.863-869.
- [6] Hirose, S., and Kunieda, O., "Generalized standard foot trajectory for a quadruped walking vehicle", Int. J. Robotics Res, (1991), pp.3-12.
- [7] Roennau, A., Kerscher, T., Dillmann, R., "Design and Kinematics of a biologically-inspired leg for a six-legged walking machine", International Conference on Biomedical Robotics and Biomechatronics, (2010), pp.626-631.
- [8] Hodoshima, R., Watanabe, S., Nishiyama, Y., Sakaki, A., and Kotosaka, S., "Development of ASURA I : Harvestman-like Hexapod Walking Robot -Approach for Long-Legged Robot and Leg Mechanism Design-", International Conference on Intelligent Robot and Systems, (2013), pp.123-127.
- [9] Sakakibara, Y., Ken, K., Hosoda, M., Hattori, M., Fujie, M., "Foot trajectory for a quadruped walking machine", International Intelligent Robots and System, (1990), pp.315-322.
- [10] Maufry, C., Nishikawa, T., and Kimura, H., "Stable dynamic walking of a quadruped robot "kotetu" using phase modulations based on leg loading/unloading", Proc. of IEEE Robotics and Automation, (2010), pp.5225-5230.

Received on December 31, 2013

Accepted on February 3, 2014